

# **MODELING THE VAPOR – LIQUID EQUILIBRIUM AND ASSOCIATION OF NITROGEN DIOXIDE / DINITROGEN TETROXIDE AND ITS MIXTURES WITH CARBON DIOXIDE**

A. Belkadi<sup>1,2</sup>, F. Llovel<sup>3</sup>, V. Gerbaud<sup>1\*</sup>, L. F. Vega<sup>2,3\*,+</sup>

<sup>1</sup>Université de Toulouse, LGC (Laboratoire de Génie Chimique), CNRS, INP, UPS, 5  
rue Paulin Talabot, F-31106 Toulouse Cedex 01 – France

<sup>2</sup>MATGAS Research Center, Campus UAB. 08193 Bellaterra, Barcelona Spain

<sup>3</sup>Institut de Ciència de Materials de Barcelona, (ICMAB-CSIC), Consejo Superior de  
Investigaciones Científicas, Campus de la UAB, 08193 Bellaterra, Barcelona, Spain

---

\* Corresponding authors: Vincent.Gerbaud@ensiacet.fr, vegal@matgas.com.

<sup>+</sup>Present address: Carburos Metálicos-Grup Air Products. C/ Aragón 300. 08009 Barcelona. Spain.

## ***Abstract***

We have used in this work the crossover soft-SAFT equation of state to model nitrogen dioxide/dinitrogen tetraoxide ( $\text{NO}_2/\text{N}_2\text{O}_4$ ), carbon dioxide ( $\text{CO}_2$ ) and their mixtures. The prediction of the vapor – liquid equilibrium of this mixture is of utmost importance to correctly assess the  $\text{NO}_2$  monomer amount that is the oxidizing agent of vegetal macromolecules in the  $\text{CO}_2 + \text{NO}_2 / \text{N}_2\text{O}_4$  reacting medium under supercritical conditions. The quadrupolar effect was explicitly considered when modeling carbon dioxide, enabling to obtain an excellent description of the vapor-liquid equilibria diagrams.  $\text{NO}_2$  was modeled as a self associating molecule with a single association site to account for the strong associating character of the  $\text{NO}_2$  molecule. Again, the vapor-liquid equilibrium of  $\text{NO}_2$  was correctly modeled. The molecular parameters were tested by accurately predicting the very few available experimental data outside the phase equilibrium. Soft-SAFT was also able to predict the degree of dimerization of  $\text{NO}_2$  (mimicking the real  $\text{NO}_2/\text{N}_2\text{O}_4$  situation), in good agreement with experimental data. Finally,  $\text{CO}_2$  and  $\text{NO}_2$  pure compound parameters were used to predict the vapor – liquid coexistence of the  $\text{CO}_2 + \text{NO}_2 / \text{N}_2\text{O}_4$  mixture at different temperatures. Experimental pressure –  $\text{CO}_2$  mass fraction isotherms recently measured were well described using a unique binary parameter, independent of the temperature, proving that the soft-SAFT model is able to capture the non-ideal behavior of the mixture.

***Keywords:*** soft-SAFT, crossover, reacting systems,  $\text{CO}_2$ ,  $\text{NO}_2 / \text{N}_2\text{O}_4$

## **1. Introduction**

Accurate thermodynamic properties of pure compounds and mixtures, in particular phase equilibrium properties, are needed over a wide range of temperatures and pressures for the optimization of existing and the design of new process and/or materials in chemical industry. Even though experimental data is always preferred, this information is often scarce and it does not cover all mixtures and operating conditions, thus inducing a persistent effort to derive accurate thermodynamic models.

From the modeling of hydrocarbon or organic compound properties needed in the petrochemical industry, and because of the advent of novel industrial technologies, a shift in modeling has occurred, focusing on uncommon fluids (ionic liquids, biomolecules, etc.) or on common fluids under severe temperature and pressure conditions, like the supercritical ones. In a comprehensive paper, Prausnitz and Tavares [1] recalled 50 years of thermodynamic models focused on vapor – liquid equilibrium. Hydrocarbons and other non polar fluid vapor – liquid equilibrium properties can be satisfactorily modeled using a symmetric approach to model both, the vapor and the liquid phase fugacity with the use of a van der Waals type equation model [2,3], the Soave – Redlich – Kwong or Peng – Robinson equations being the most popular ones. When polar fluids are involved at moderate pressures, activity coefficient models are more suitable for modeling the liquid phase. When a higher pressure range is also a concern, a symmetric equation of state approach with complex mixing rules including an excess Gibbs energy term from an activity coefficient model can provide good results. Unfortunately, even those approaches show limitations for complex fluids and can drastically fail near the critical region, unless an specific treatment is included [4,5].

For self-associating fluids like carboxylic acids, alkanols or primary and secondary amines, practical thermodynamic modeling has suggested the description of the dimer – monomer association equilibrium in the relevant phase in order to correct the monomer composition participating into the vapor – liquid phase equilibrium. This is the case for acetic acid, a molecule that dimerizes mostly in the vapor phase [6,7]. Self-associating fluids in the liquid phase are not so frequent but do exist, like  $\text{NO}_2$ , which forms  $\text{N}_2\text{O}_4$  dimers in the liquid phase [8].

In the recent decades, progress in computer science has enabled molecular simulations to solve real problems, like the prediction of vapor – liquid equilibrium of highly non ideal complex mixtures, by the use of statistical mechanic principles, developing efficient bias to sample fluid configurations [9,10]. However, although the large computational time of the molecular simulation is not prohibitory to obtain thermodynamic properties that are hardly measurable, it still prevents its use in practical and fast chemical engineering calculations.

Molecular based equations of state also rooted in statistical mechanics, are a very attractive alternative. They retain their interest in chemical engineering calculations as they apply to a wide spectrum of thermodynamic conditions and compounds, being computationally much less demanding than molecular simulations. Among them, the Statistical Associating Fluid Theory equation of state (SAFT) has become very popular because of its capability of predicting thermodynamics properties of several complex fluids, including chain, aromatic and chlorinated hydrocarbons, esters alkanols, carboxylic acids, etc [11]. SAFT was envisioned as an application of Wertheim's theory of association [12-14] through the use of a first order thermodynamic perturbation theory (TPT) to formulate a physically based EoS [11, 15-

17] The ambition of making SAFT an accurate equation for engineering purposes has promoted the development of different versions that tried to overcome the limitations of the original one [18,19].

The objective of this paper is to check the accuracy of one of these approaches for describing the vapor-liquid equilibrium diagrams and association of the  $\text{CO}_2 + \text{NO}_2 / \text{N}_2\text{O}_4$  mixture. The prediction of the vapor – liquid equilibrium of this mixture is of utmost importance to correctly assess the  $\text{NO}_2$  monomer amount that is the oxidizing agent of vegetal macromolecules in the  $\text{CO}_2 + \text{NO}_2 / \text{N}_2\text{O}_4$  reacting medium. Such a mixture is the reacting media in a novel process where body-degradable polymers readily usable for inside body surgery treatment are produced through the oxidation of polysaccharides and cellulose macromolecules by  $\text{NO}_2/\text{N}_2\text{O}_4$  in a reactor where  $\text{CO}_2$  is present in excess under supercritical conditions [20]. Currently, the oxidizing agent is suspected to be  $\text{NO}_2$  monomers but a real assessment of its exact quantity in the reacting medium is missing to further optimize the process conditions.

Supercritical  $\text{CO}_2$  is now well established as a solvent for use in extractions. The modeling of  $\text{CO}_2$  is routinely done using cubic equation of state. However,  $\text{CO}_2$  bears a quadrupole that, if not considered in the modeling, provides inaccurate mixture predictions that have to be corrected by the use of binary interaction parameters [21]. A recent modeling of  $\text{CO}_2$  – perfluoroalkanes vapor – liquid equilibrium mixtures using the soft-SAFT equation of state showed that no binary interaction parameters are required when the quadrupolar moment on carbon dioxide is explicitly included and molecules do not greatly differ in size. In that case, the quadrupolar effect on the phase

equilibrium is not hidden in the binary parameter value but explicitly described increasing the model extrapolation capability [21].

The oxides of nitrogen are of main interest, notably for their occurrence in biological and environmental chemistry. Nitrogen dioxide ( $\text{NO}_2$ ) is notoriously known to self associate in the liquid phase to produce dinitrogen tetroxide ( $\text{N}_2\text{O}_4$ ) according to Equation 1 [8]. In the liquid phase,  $\text{N}_2\text{O}_4$  can also additionally isomerizes [22]. In the vapor phase, it was shown that dimerization also occurs, while the formation of trimers, tetramers or sequential indefinite self-association hypothesis can be discarded [23]. In this work  $\text{NO}_2$  is modeled as a self associating molecule with a single association site to account for the strong associating character of the  $\text{NO}_2$  molecule. Assuming that the self associating compound  $\text{NO}_2$  is a mixture of monomers  $\text{NO}_2$  and dimers  $\text{N}_2\text{O}_4$ , the dissociation reaction to be considered is:



According to interpretation of Raman and X-ray spectra [24] and the most recent computational chemistry study [25], it has been confirmed that the  $\text{NO}_2$  association takes place along the NN bond line. Both  $\text{NO}_2$  and  $\text{N}_2\text{O}_4$  molecules are fairly rigid.

Hence, in spite of its importance and given the non-ideal behavior of the components, the  $\text{CO}_2 + \text{NO}_2 / \text{N}_2\text{O}_4$  mixture is a challenging mixture to model. The approach we have taken here is to use the soft-SAFT equation of state [26,27], as it explicitly builds on the association and the quadrupolar interactions. Therefore, the equation is able to provide insights on the mixture behavior, as for instance, the degree of aggregation of associating molecules in each phase in equilibrium [28]. Like most

thermodynamic models, SAFT approaches require the evaluation of several parameters relating the model to the experimental system. An advantage of SAFT-type equations versus other approaches is that, as they are based on statistical mechanics, parameters have a clear physical meaning; when carefully fitted they can be used with predictive power to explore other regions of the phase diagram far from the data and operating conditions used in the parameter regression, performing better than other models for interacting compounds like activity coefficient models [1]. Modeling predictions are compared to very recent experimental measurements of  $\text{NO}_2 - \text{CO}_2$  equilibrium isotherms [29].

The paper is organized as it follows: first, the crossover soft-SAFT equation of state is shortly described, including the molecular model used for  $\text{CO}_2$  and  $\text{NO}_2$ . In the results section, the soft-SAFT equation results are presented and discussed, as compared to available experimental data, phase envelopes of the pure compounds, additional thermodynamic data of  $\text{NO}_2$  (used to validate the pure component parameters), degree of dimerization for the  $\text{NO}_2/\text{N}_2\text{O}_4$  system, and the mixture  $\text{CO}_2 + \text{NO}_2 / \text{N}_2\text{O}_4$ . Some concluding remarks are provided in the last section.

## ***2. The crossover soft-SAFT equation of state***

The soft-SAFT EoS [26] is a modification of the original SAFT equation [15-17], based on Wertheim's TPT [12-14]. Since the SAFT equation and its modifications have been extensively revised [19], only the main features of the equation are retained here. SAFT-type equations of state are written in terms of the residual Helmholtz energy:

$$a^{res} = a - a^{id} = a^{ref} + a^{chain} + a^{assoc} + a^{polar} \quad (2)$$

where  $a$  and  $a^{id}$  are the total Helmholtz energy density and the ideal gas Helmholtz energy density at the same temperature and density, respectively.  $a^{ref}$  is the contribution to the Helmholtz energy of the spheres term composing the molecules;  $a^{chain}$ , the chain contribution term and  $a^{assoc}$ , the association term, both come from Wertheim's theory. Finally,  $a^{polar}$  takes into account the polar contribution to the Helmholtz energy. In essence, in the SAFT approach the total Helmholtz energy is the sum of different microscopic contributions, all of which can be taken into account in a systematic manner.

The main difference between the soft-SAFT equation and the original SAFT equation [15-17] is the use of the Lennard–Jones (LJ) intermolecular potential for the reference fluid in the soft-SAFT equation, with dispersive and repulsive forces into the same term, instead of the perturbation scheme based on a hard-sphere reference fluid plus dispersive contributions to it. This difference also appears in the chain and association term, since they both use the radial distribution function of the reference fluid, and it has turned out to be relevant for some applications of the equation.

Hence, the reference term in the soft-SAFT EOS is a LJ spherical fluid, which represents the units making up the chains. Following our previous work, we have used the accurate EoS of Johnson et al. [30]. The chain term in the equation comes from Wertheim's theory, and it is formally identical in the different versions of SAFT. It is expressed as:



$$a^{chain} = \rho \ k_B T \sum_i x_i (1 - m_i) \ln g_{LJ} \quad (3)$$

where  $\rho$  is the molecular density of the fluid,  $T$  is the temperature and  $k_B$  is the Boltzmann constant. In the soft-SAFT case, it is applied to tangent LJ spheres of chain length  $m$  that are computed following a pair correlation function  $g_{LJ}$ , evaluated at the bond length  $\sigma$ .

The association term comes from the first-order Wertheim's TPT for associating fluids, The Helmholtz energy density change due to association is calculated from the equation

$$a^{assoc} = \rho \ k_B T \sum_i x_i \sum_{\alpha} \left( \ln X_i^{\alpha} - \frac{X_i^{\alpha}}{2} \right) + \frac{M_i}{2} \quad (4)$$

where  $M_i$  is the number of associating sites of component  $i$  and  $X_i^{\alpha}$  the mole fraction of component  $i$  not bonded at site  $\alpha$  which accounts for the contributions of all associating sites in each species:

$$X_i^{\alpha} = \frac{1}{1 + N_{avog} \rho \sum_j x_j \sum_{\beta} X_j^{\beta} \Delta^{\alpha\beta}_{ij}} \quad (5)$$

The term  $\Delta^{\alpha\beta}_{ij}$  is related to the strength of the association bond between site  $\alpha$  in molecule  $i$  and site  $\beta$  in molecule  $j$ , from which two additional molecular parameters, related to the association, appear:  $\epsilon^{\alpha\beta}_{ij}$ , the association energy and  $\kappa^{\alpha\beta}_{ij}$ , the

association volume for each association site and compound, (see, for instance, ref [26] for details)

The extension of the equation to polar systems is done by adding a new contribution that consists in a perturbed polar term proposed by Gubbins and Twu [31].

$$a^{qq} = a_2^{qq} \left[ \frac{1}{1 - \left( \frac{a_3^{qq}}{a_2^{qq}} \right)} \right] \quad (6)$$

Expressions for  $a_2^{polar}$  and,  $a_3^{polar}$ , the second and third-order perturbation terms, were derived for an arbitrary intermolecular reference potential and can be found in the original papers [32-33]. These expressions include the polar moment of the molecule ( $Q$  for the quadrupole case, which is the one evaluated in this work [34]), whose value is taken from experimental measurements.

Since the reference term is written and established for a pure compound (in contrast with the chain, association or polar terms, which are directly applicable to mixtures), the residual Helmholtz energy density of the mixture is approximated by the residual Helmholtz energy density of a pure hypothetical fluid, using the van der Waals one fluid theory:

$$\sigma^3 = \frac{\sum_i \sum_j x_i x_j m_i m_j \sigma_{ij}^3}{\left( \sum_i x_i m_i \right)^2} \quad (7)$$

$$\varepsilon\sigma^3 = \frac{\sum_i \sum_j x_i x_j m_i m_j \varepsilon_{ij} \sigma_{ij}^3}{\left(\sum_i x_i m_i\right)^2} \quad (8)$$

$$m = \sum_i x_i m_i \quad (9)$$

The above equations involve the mole fraction  $x_i$  and the chain length  $m_i$  of each of the components of the mixture of chain. The crossed interaction parameters  $\sigma_{ij}$  and  $\varepsilon_{ij}$  are calculated using the generalized Lorentz-Berthelot mixing rules:

$$\sigma_{ij} = \eta_{ij} \frac{\sigma_{ii} + \sigma_{jj}}{2} \quad (10)$$

$$\varepsilon_{ij} = \xi_{ij} \sqrt{\varepsilon_{ii} \varepsilon_{jj}} \quad (11)$$

where  $\eta_{ij}$  and  $\xi_{ij}$  represent the fitting parameters for binary mixtures deviating from ideal behavior, corresponding to a size and energy parameter, respectively. In this sense,  $\eta_{ij}$  and  $\xi_{ij}$  equal to one means full predictions from pure component parameters. In this work we have used just one binary parameter,  $\xi_{ij}$  with a value very close to unity.

An extension of the original equation includes the addition of a crossover treatment to take into account the contribution of the long-wavelength density fluctuations in the near critical region, the so-called crossover soft-SAFT EOS [4]. Based on White's work [35], from the Wilson's renormalization group theory [36], this term is implemented by using recursive relations where the density fluctuations are successively incorporated. This is the generalized equation we have used along the

present work. The Helmholtz energy density of a system at density  $\rho$  can be described in recursive manner as:

$$a^{total} = \sum_{n=1}^{\infty} a_n(\rho) = \sum_{n=1}^{\infty} [a_{n-1}(\rho) + da_n(\rho)] \quad (12)$$

where  $a_n$  is the Helmholtz energy density and  $da_n$  the term where long wavelength fluctuations are accounted for in the following way:

$$da_n(\rho) = -K_n \frac{\Omega^s(\rho)}{\Omega^l(\rho)} \quad (13)$$

where  $\Omega^s$  and  $\Omega^l$  represent the density fluctuations for the short-range and the long-range attraction respectively, and  $K_n$  is a coefficient that depends on the temperature and the cut off length:

$$K_n = \frac{k_B T}{2^{3n} \cdot L^3} \quad (14)$$

$$\Omega_n^\beta(\rho) = \int_0^\rho \exp\left(\frac{-G_n^\beta(\rho, x)}{K_n}\right) dx \quad (15)$$

$$G_n^\beta(\rho, x) = \frac{\bar{a}_n^\beta(\rho + x) + \bar{a}_n^\beta(\rho - x) - 2\bar{a}_n^\beta(\rho)}{2} \quad (16)$$

The superindex  $\beta$  refers to both long ( $l$ ) and short ( $s$ ) range attraction, respectively, and  $G^\beta$  is a function that depends on the evaluation of the function  $\bar{a}$ , calculated as:

$$\bar{a}_n^l(\rho) = a_{n-1}(\rho) + \alpha \cdot (m \cdot \rho)^2 \quad (17)$$

$$\bar{a}_n^s(\rho) = a_{n-1}(\rho) + \alpha \cdot (m \cdot \rho)^2 \cdot \frac{\phi \cdot w^2}{2^{2n+1} \cdot L^2} \quad (18)$$

where  $m$  is the chain length (number of LJ segments forming the chain),  $\phi$  is an adjustable parameter,  $\alpha$  is the interaction volume with units of energy-volume, and  $w$  refers to the range of the attractive potential. The values of  $\alpha$  and  $w$  for the LJ potential were provided by Llovell and Vega [37].

The extension to mixtures is done following the isomorphism assumption, in the same way as Cai and Prausnitz [38]. Following this approach the one-component density is replaced by the total density of the mixture. In addition, calculations are further simplified by using Kiselev and Friend's approximation [39], in which chemical potentials are replaced by mole fractions as independent variables. Finally, the mixing rules needed to determine the crossover parameters  $L$  and  $\phi$  are defined as in previous works [5,37]:

$$L^3 = \sum_{i=1}^n x_i L_i^3 \quad (19)$$

$$\phi = \sum_{i=1}^n x_i \phi_i \quad (20)$$

For practical applications, the summation in equation 12 is extended to five iterations, because no further changes in the properties are observed.

The soft-SAFT EoS needs a minimum of three pure compound parameters to model any non spherical molecule:  $m$ , the chain length,  $\sigma$  the diameter of the LJ spheres forming the chain, and  $\varepsilon$  the interaction energy between the spheres. For associating molecules, the association volume  $\kappa^{HB}$  and the association energy  $\varepsilon^{HB}$  of the sites of the molecule should be considered; for polar molecules the polar moment (that can be dipolar, quadrupolar or octopolar, depending on the structure) can be explicitly included. These parameters are treated as adjustable when applying the equation for real fluids, although some clear trends within chemical families have been found. The inclusion of the crossover treatment leads to two additional parameters, the *cutoff* length  $L$ , related to the maximum wavelength fluctuations that are accounted for the uncorrected free energy, and  $\phi$ , the average gradient of the wavelet function, used as an adjustable parameter. Finally, when dealing with non ideal mixtures, binary interaction parameters  $\eta$  and  $\zeta$  are sometimes required. In our case only  $\zeta$  is used.

In this work the CO<sub>2</sub> molecule was modeled as a fully flexible LJ chain of length  $m$ , where the quadrupole was explicitly taken into account. The molecular parameters are:  $m$ , the chain length;  $\sigma$ , the size parameter;  $\varepsilon$ , the energy parameter, the quadrupolar moment  $Q$  and the  $x_p$  fraction of segments that contains the quadrupole. NO<sub>2</sub> was also modeled as a fully flexible LJ chain of length  $m$ , with  $\sigma$  and  $\varepsilon$  as the size and energy parameters, respectively; to mimic the strong associating character of this fluid, an associating site was also included in this case, with two additional parameters,  $\varepsilon^{HB}$  and  $\kappa^{HB}$ , representing the energy and volume of association per site.

All parameter values were obtained by fitting experimental saturated liquid densities and vapor pressures for each component by minimizing the following objective function:

$$F_{obj}^{corps} = \frac{1}{N^P} \sum_{i=1}^{N_P} \left( \frac{Y_i^{cal} - Y_i^{exp}}{Y_i^{exp}} \right)^2 \quad (21)$$

where  $Y$  represents the property data used for the regression, namely  $\rho^{liq}$  and  $P^{sat}$ .

### 3. Results and discussion

#### 3.1. Pure compounds VLE modeling

The soft-SAFT equation of state described above was used with parameters presented in Table 1. Figure 1 depicts the phase diagram of carbon dioxide as obtained with three sets of parameters as compared to experimental data [40]. The third set of parameters in table 1 (dotted lines in figure 1) corresponds to optimized parameters from the original equation, without including the crossover term, as obtained by Dias et al.[21]. These parameters were optimized to best fit the phase diagram, except the critical region. The first set of parameters in table 1 were optimized in the present work when applying the crossover soft-SAFT equation to the same set of experimental data as in Dias et al. [21] (full lines in figure 1). Thanks to the crossover treatment, the overall curve is very well reproduced, including the critical region. Finally, a third set of parameters was used for comparison: the dashed lines correspond to calculations performed with the original soft-SAFT equation, that is without crossover but with the

$m$ ,  $\sigma$  and  $\varepsilon$  values fitted when using the crossover treatment. In that case, agreement is similar to the one obtained with Dias's parameter set without crossover but, as this second parameter set was not refitted, it deviates more in the liquid phase; a fact already pointed out by Llovell et al. [5]. Quadrupolar interactions were explicitly considered in all cases with quadrupolar parameter  $Q$  taken from the value fitted by Dias et al. [21] which compared well with experimental values of the  $\text{CO}_2$  quadrupole. The value of the calculated critical points are presented in the Table 2; stressing the excellent agreement achieved thanks to the crossover treatment.

$\text{NO}_2$  is a strongly associating molecule, mostly appearing with its dimer in the liquid phase. The  $\text{NO}_2/\text{N}_2\text{O}_4$  molecule was already studied by De Souza and Deiters [42], modeling its VLE by the use of two different molecular based EoS: the Hard Sphere Attractive (HSA) EoS and the Semi empirical EoS (SES). In the first equation HSA, molecules were modeled as single hard spheres / beads with a mean field – type attraction. Two adjustable parameters were needed: the hard sphere diameter and the attractive interaction parameter. The second formulation, SES, had three adjustable molecular parameters (molecule size, attractive energy, and anisotropy parameter). Unsurprisingly, SES, with its adjustable anisotropic parameter, gave better overall results. As these equations did not include any specific treatment for critical region calculations, the approach failed to match the critical temperature of  $\text{NO}_2$  by more than 10 K, while the experimental dissociation constant differed by -25% (HSA) and +5% (SES) respect to the experimental values. Modeling of binary mixtures  $\text{NO}_2 + \text{CCl}_4$  and  $\text{NO}_2 + \text{cyclohexane}$  gave reasonable results with the same trends for the dissociation constant than for pure  $\text{NO}_2$ .



In our case the molecule of NO<sub>2</sub> was modeled as an associating molecule with one site of association located at the N atom. From the observations of Huang and Radosz [11] about the relation between the association strength  $\epsilon^{HB}$  and volume  $\kappa^{HB}$  value, NO<sub>2</sub> can be classified as a strong associating fluid, in agreement with experimental observations. In our modeling approach this translate into a large  $\epsilon^{HB}$  value and a small  $\kappa^{HB}$  value. The association volume is significantly smaller than for moderately associating fluids (alkanols) modeled with the soft-SAFT equation [37]. Contrary to the association in alkanols, or even in carboxylic acid dimers that corresponds to loose hydrogen bonds from 2.1 to 2.8 Å, chemical association in the NO<sub>2</sub> corresponds to a shorter and stronger bond (1.78 Å according to Chesnut and Crumbliss [25]). The molecular parameters of NO<sub>2</sub> are optimized with the crossover soft-SAFT EoS and also used as is with the classical soft-SAFT EoS leading to two parameter sets in table 1. As both set of parameters give accurate results in the subcritical region, no optimized parameters for the classical soft-SAFT equation were further sought.

Figure 2 depicts the vapor-liquid equilibrium of NO<sub>2</sub>. Figure 2a shows the temperature-density diagram while Figure 2b is devoted to the pressure-temperature diagram. The experimental density data in the vapor-liquid coexistence region was taken from the work of Reamer and Sage [43]. Additional low temperature liquid density data were taken from Gray and Rathbone [44] and saturated pressure data at low temperature was taken from Giaume and Kemp [24]. In both graphs we compare the performance of the soft-SAFT equation with (full line) and without (dashed line) the crossover treatment with the parameters given in table 1. Unlike CO<sub>2</sub> where use of crossover fitted parameters in the equation without crossover led to increased deviation in the liquid density, both NO<sub>2</sub> sets performed equally well far from the critical region,

probably due to the strong influence association plays in this compound. The crossover term makes the agreement with the experimental phase diagram to become excellent over the whole phase region including the critical region.

The molecular parameters obtained by fitting vapor – liquid equilibrium data were used to check their transferability for other regions of the phase diagram not included in the fitting procedure but for which there is available data. Figure 3 shows the variation of the predicted liquid density versus the total pressure of the system at two isotherms (294.3K and 360.9K), as compared to experimental data. As it can be observed, the model is in very good agreement with the experimental data [43]. It also performs better than both SES and HAS models [42] that deviated much more at high pressures, in particular SES for the 360.9 K measurements and HSA for the 294.3 K measurements. The difference between the soft-SAFT equation with and without crossover displayed in figure 3 exists but is not significant, as expected at such a subcritical temperature.

In addition to obtaining accurate phase diagrams, the use of soft-SAFT enables to evaluate the fraction of dimerization in the  $\text{NO}_2$  molecule, since the association term, leading to the dimer formation, is built into the theory. Experimental monomer  $\text{NO}_2$  fractions in the liquid phase data is scarce and concerns only the low temperature range 246.65 – 295.95 K [8]. The crossover soft SAFT predicts about 40% of  $\text{NO}_2$  monomer (50% without crossover) at the calculated critical temperature and reaches a maximum of 53% (58% without crossover) (Figure 4a). Indeed, the maximum mole fraction of monomer  $\text{NO}_2$  in the mixture is not achieved at the critical temperature. It is observed that a high temperature favors the monomer  $\text{NO}_2$  (from the non-interacting, ideal part of

the energy change upon reaction) whereas high pressure favors  $\text{N}_2\text{O}_4$  (because of the stoichiometry  $\text{N}_2\text{O}_4:\text{NO}_2$ ). The balance between those two forces is observed in Figure 4a. The curves are similar to those obtained by De Souza and Deiters [42] for their SES and HSA EoSs. Those authors also computed the theoretical monomer fraction assuming ideal gas and liquid and taking densities from the SES EoS. The shape of all curves is similar but the effect of non-ideality is evident in the liquid phase, where it contributes to a lower mole fraction of  $\text{NO}_2$  than what would be expected from purely ideal calculations. A zoom on the experimental data (Figure 4b) shows a discrepancy with the predictions at low temperature. Calculations and experimental points of James and Marshall [7] differ by an order of magnitude but the absolute value of the non bonded  $\text{NO}_2$  remains extremely small.

Figure 5 shows the molar fraction of non bonded  $\text{NO}_2$  in the vapor phase versus the pressure at 293.15 K. Circles represent experimental data from Yoshino *et al.* [45] while the line is the crossover soft-SAFT EoS prediction. The agreement obtained between the experimental measurements and the theory is within the experimental uncertainty, further reassuring the validity of soft-SAFT for these systems.

A large number of dissociation constants are available in the literature, especially in the gas phase. Figure 6 compares the calculated values with experimental data from Dunn *et al.* [46] that also compared well with previous measurements [24,47]. The crossover equation reproduces the experimental data quite accurately, with the largest deviations at high pressure and temperature.

Overall, modeling of  $\text{NO}_2$  using the crossover soft-SAFT EoS nicely reproduces the main features of the experimental data available in the literature, and it improves the

former modeling that used a hard sphere equations of state HSA and a semi-empirical equation of state SES [42].

### 3.2 CO<sub>2</sub> + NO<sub>2</sub> / N<sub>2</sub>O<sub>4</sub> mixture VLE modeling

The next step in this work concerned the evaluation of the mixture CO<sub>2</sub> + NO<sub>2</sub> / N<sub>2</sub>O<sub>4</sub>. The previously mentioned pure compound parameters were used to predict the vapor – liquid coexistence of the mixture. The only experimental data available for this mixture is related to a recent work of Camy *et al.* [29], who have measured the pressure versus the CO<sub>2</sub> mass fraction at several temperatures. Those authors have estimated an absolute measurement error of  $\Delta x_{\text{CO}_2}=0.036$  to the mass fraction of CO<sub>2</sub> and  $\Delta P=0.075\text{MPa}$ . At first, pure predictions from crossover soft-SAFT without binary interaction parameters were attempted; although the EoS captured the shape of the curve, it failed to give an accurate description of the experimental data. The use of a unique binary parameter  $\zeta_{ij}$  was introduced by fitting the experimental data of the isotherm at 313K (which is the only one with enough experimental information to perform satisfactory regression) to the absolute average deviation on pressure computed from equation 22. Calculations are presented in the Table 3.

$$AADP = \frac{100}{N^p} \sum_1^{N^p} \left( \frac{P^{cal} - P^{exp}}{P^{exp}} \right)^2 \quad (22)$$

Figure 7 shows a pressure-composition diagram of this mixture at three different temperatures, from 298 till 328K. Symbols represent the experimental information

measured by Camy et al. [29], while the full lines are the crossover soft-SAFT calculations. The dotted-dashed line represents the critical line.

We note that all calculations of those isotherms were done with the mass fraction of  $\text{CO}_2$  not as usually done with the molar fraction. For such systems containing reacting system it is better to use the monomer as a reference molecule and its non bonded fraction in the mixture  $X$ , in our case provided by the crossover soft-SAFT EoS. The binary parameter value obtained ( $\xi = 1.045$ ) was enough to give quantitative agreement for the whole composition range. Although regressed on the 313.15K isotherm, it predicts as well the behavior of the other isotherms and the critical line. The very few experimental points at the other temperatures do not permit to give a clear conclusion about the agreement with the experimental work. It seems clear that more measurements are needed to extract a clear conclusion about the modeling.

#### **4. Conclusions**

The crossover soft-SAFT equation of state has been used to successfully describe the  $\text{CO}_2 + \text{NO}_2 / \text{N}_2\text{O}_4$  vapor – liquid equilibrium properties, as well as the pure component phase equilibria. The prediction of  $\text{CO}_2 + \text{NO}_2 / \text{N}_2\text{O}_4$  vapor – liquid equilibrium properties is of utmost importance to assess correctly the  $\text{NO}_2$  monomer amount that is the oxidizing agent of cellulose in the  $\text{CO}_2 + \text{NO}_2 / \text{N}_2\text{O}_4$  reacting medium, leading to the production of body-degradable polymers readily usable for inside body surgery.

CO<sub>2</sub> parameters were regressed following the same procedure as Llovell and Vega [37] and Dias et al. [21] but refining their optimization so as to improve the liquid phase density; the quadrupolar interactions were explicitly considered. NO<sub>2</sub> was treated as a self associating compound with a single association site. Compared to other self associating fluids, the large  $\epsilon^{HB}$  and small  $\kappa^{HB}$  optimized values defined NO<sub>2</sub> as a strong associating fluid, in agreement with the experimental observations. The association volume  $\kappa^{HB}$  found is significantly smaller than that used for moderately associating fluids (alkanols) modeled with the same crossover soft-SAFT equation [37]. The proposed model and parameters fitted to vapor liquid equilibria was used to predict liquid density value at two temperatures, showing very good agreement with experimental data and improving the performances of previous published models [42].

The NO<sub>2</sub> modeling included a study of the dimerization fraction of the molecule. Crossover soft-SAFT predicted a maximum dimerization fraction of 53%. Moreover, the equation showed good agreement when compared to the very few experimental data available, concerning the dimerization fraction at room temperature and the evaluation of the dissociation constant value.

Finally, crossover soft-SAFT was used to evaluate the vapor – liquid coexistence of CO<sub>2</sub> + NO<sub>2</sub> / N<sub>2</sub>O<sub>4</sub> mixture and its critical line, using the pure component molecular parameters. Experimental pressure – CO<sub>2</sub> mass fraction isotherms recently measured were used for comparison [29]. The use of a unique constant binary parameter was enough to achieve good agreement respect to the experimental data, although more experimental information would be required to assure the validity of the mixture calculations. In any case, results for pure compounds indicate that crossover soft-SAFT

provides a rigorous model that can be applied to study this mixture with a good degree of accuracy.

## ACKNOWLEDGEMENTS

A. Belkadi acknowledges the Ministère de l'Enseignement Supérieur et de la Recherche de France (MESR) for its grants and the CTP 2005 project (Convention Région N° 05018784). This research has been possible due to the financial support received from the Spanish Government (project CTQ2005-00296/PPQ), and from the Generalitat de Catalunya (2005SGR-00288 and project ITT2005-6/10.05). We are thankful to S. Camy, J.J. Letourneau and J.S. Condoret for providing their experimental data for the mixtures. This work was partially accomplished during two short stays of A. Belkadi at the ICMAB and MATGAS laboratories.

### *List of symbols*

*AADP* Absolute average deviation from the pressure

$a$  Helmholtz energy density (mol/L) and vdW attractive parameter

$g$  radial distribution function

$k_B$  Boltzmann constant (J/K)

$K$  equilibrium constant

$L$  cutoff length in the crossover soft-SAFT equation (m)

$m$  chain length parameter for the soft-SAFT equation

*Navog* Avogadro's Number

$N_p$  Number of experimental points

$P$  pressure (bar)

$Q$	quadrupolar moment
$T$	absolute temperature (K)
$w$	range of the attractive potential
$x$	integral variable, molar composition
$x_p$	fraction of segment that take into account the quadrupolar moment
$X$	fraction of not bonded molecules
$y$	molar composition

#### *Greek letters*

$\mu$	chemical potential
$\rho$	phase density (mol/L)
$\phi$	crossover constant
$\Omega$	density fluctuation for the short-range and the long-range attraction.
$\alpha$	associating site, interaction volume in the crossover term
$\beta$	associating site
$\sigma$	segment diameter parameter for the soft-SAFT equation
$\varepsilon$	dispersive energy parameter for the soft-SAFT equation
$\nu$	stoichiometric coefficient
$\kappa^{HB}$	volume of association parameter for the soft-SAFT equation
$\varepsilon^{HB}$	energy of association parameter for the soft-SAFT equation
$\Delta$	related to the strength of the association interaction

#### *Subscripts*

$0$	zero-order variation
$c$	critical
$i$	constituent reference
$max$	maximum
$min$	minimum
$n$	nth-order variation
$r$	reduced



### *Superscripts*

<i>s</i>	short-range attraction
<i>l</i>	long-range attraction
$\beta$	short or long-range attraction
<i>assoc</i>	association
<i>cal</i>	calculated
<i>chain</i>	chain
<i>exp</i>	experimental
<i>id</i>	ideal
<i>LJ</i>	Lennard-Jones
<i>polar</i>	polar
<i>qq</i>	quadrupolar
<i>ref</i>	reference

### **References**

- [1] J. M. Prausnitz, F. W. Tavares, AIChE Journal. 50 (4) (2004) 739-761.
- [2] H. Segura, D. Seiltgens, A. Mejia, F. Llorell, L.F. Vega, Fluid Phase Equilibria (submitted).
- [3] H. Segura, D. Seiltgens, A. Mejia, F. Llorell, L.F. Vega, Fluid Phase Equilibria (submitted).
- [4] F. Llorell, L.F. Vega, D. Seiltgens, A. Mejía, H. Segura, Fluid Phase Equilibria (2007) in press.
- [5] F. Llorell, J.C. Pàmies, L.F. Vega, Journal of Chemical Physics. 121 (21) (2004), 10715-10724.
- [6] J. Marek, Collection of Czechoslovak Chemical Communications. 19 (5) (1954) 1074-1081.

- [7] J. Marek, Collection of Czechoslovak Chemical Communications. 20 (6) (1955), 1490-1502.
- [8] D. W. James, R. C. Marshall, J. Phys. Chem. 72 (1968) 2963-2966.
- [9] M.P. Allen, D.J. Tildesley, *Computer Simulation of Liquids*, Oxford University Press, New York, United Kingdom, 1987.
- [10] J.J. De Pablo, F.A. Escobedo, AIChE Journal. 48 (12) (2002) 2716-2721.
- [11] S. H. Huang, M. Radosz, Ind. Eng. Chem. Res. 29 (1990) 2284-2294.
- [12] M. S. Wertheim, J. Stat. Phys. 35 (1-2) (1984) 19-34.
- [13] M. S. Wertheim, J. Stat. Phys. 35 (1-2) 1984, 35-47.
- [14] M. S. Wertheim, J. Stat. Phys. 42 (3-4) (1986) 459-476.
- [15] W. G. Chapman, G. Jackson, K. E. Gubbins, Mol. Phys. 65 (1988) 1057-1079.
- [16] W. G. Chapman, K. E. Gubbins, G. Jackson, M. Radosz, Ind. Eng. Chem. Res. 29 (1990), 1709-1721.
- [17] S. H. Huang, M. Radosz, Ind. Eng. Chem. Res. 30 (1991) 1994-2005.
- [18] E. A. Müller, K.E. Gubbins, Ind. Eng. Chem. Res. 34 (1995) 3662-3673.
- [19] I. G. Economou, Ind. Eng. Chem. Res. 41 (2002) 953-962.
- [20] M. Vignon, S. Montanari, D. Samain, J. S. Condoret, *Procédé d'Oxydation contrôlée de Polysaccharides*, Patent n°2.873.700, FR 04 08402, 29/07/04, 2004.
- [21] A. M. A. Dias, H. Carrier, J. L. Daridon, J. C. Pàmies, L. F. Vega, J. A. P. Coutinho, I. M. Marrucho, Ind. Eng. Chem. Res. 45 (2006) 2341-2350.
- [22] D. A. Pinnik, S. F. Agnew, B. I. Swason, J. Phys. Chem. 96 (1992) 7092-7096.
- [23] D. R. Powell, E.T. Adams Jr, J. Phys. Chem. 82 (17) (1978) 1947-1952.
- [24] W. F. Giaque, J. D. Kemp, J. Chem. Phys. 6 (1) (1938) 40-52.
- [25] D.B. Chesnut, A.L. Crumbliss, Chemical Physics. 315 (2005) 53-58.
- [26] F. J. Blas, L. F. Vega, Molec. Phys. 92 (1997) 135-150.
- [27] F.J. Blas, L.F. Vega, Ind. Eng. Chem. Res. 37 (1998) 660-674.

- [28] C. Herdes, J.C. Pàmies, R.M. Marcos, L.F. Vega, J. Chem. Phys. 120 (2004) 9822-9830.
- [29] S. Camy , J.J. Letourneau, J.S. Condoret, private communication, 2007.
- [30] J.K. Johnson, J.A. Zollweg, K. E. Gubbins, Molec. Phys. 78 (1993) 591-618.
- [31] K. E. Gubbins, C. H. Twu, Chemical Engineering Science. 33 (7) (1978) 863-878.
- [32] W. Cong, Y. Li, J. Lu, Fluid Phase Equilibria. 124 (1-2) (1996) 55-65.
- [33] J. C. Liu, J.F. Lu, Y.G. Li, Fluid Phase Equilibria. 142 (1-2) (1998) 67-82.
- [34] N. Pedrosa, J. C. Pàmies, J. A. P. Coutinho, I. M. Marrucho, and L. F. Vega, Ind. Eng. Chem. Res. 44 (2005) 7027-7037.
- [35] A. White, Fluid Phase Equilibria. 75 (1992) 53-64.
- [36] K. G. Wilson, Phy. Rev. B. 4 (1971) 3174-3183.
- [37] F. Llorell, L.F. Vega, J. Phys. Chem. B. 121 (110) (2006) 1350-1362.
- [38] J. Cai, J. M. Prausnitz, Fluid Phase Equilibria. 219 (2004) 205-217.
- [39] S. Kiselev and D. Friend, Fluid Phase Equilibria. 162 (1999) 51-82.
- [40] NIST Chemistry Webbook, <http://webbook.nist.gov/chemistry>
- [41] C. M. Colina, A. Galindo, F. J. Blas, K. E. Gubbins, Fluid Phase Equilibria. 222 (2002) 77-85.
- [42] L.E.S De Souza, U.K. Deiters, Phys. Chem. Chem. Phys. 2 (2000) 5606-5613.
- [43] H. H. Reamer, B.H. Sage, Ind. Eng. Chem. Res. 44 (1) (1952) 185-187.
- [44] P. Gray, P. Rathbone, J. Chem. Soc. (1958) 3550-3557.
- [45] K. Yoshino, J. R. Esmond, W.H. Parkinson, Chem. Phys. 221 (1997) 169-174.
- [46] M. G. Dunn, K. Wark Jr, J.T. Agnew, Journal Of Chemical Physics, 37 (10) (1962) 2445-2448.
- [47] F. H. Verhoek, F. Daniels, J. Am. Chem. Soc. 53 (1931) 1250-1263.

## List of figure captions

**Figure 1** **a)** Temperature-density and **b)** pressure-temperature diagram of carbon dioxide. The dotted lines represent calculations from the original soft-SAFT with optimized parameters for this version from Dias et al. [21], the full line stands for the crossover soft-SAFT equation with optimized parameters and the dashed lines calculations with the original soft-SAFT equation with the same  $m$ ,  $\sigma$  and  $\varepsilon$  values optimized with the crossover equation. See text for details. The symbols are the NIST data taken from [40].

**Figure 2** **a)** Temperature-density and **b)** pressure-temperature diagram of the reacting system nitrogen dioxide / dinitrogen tetroxide. The dashed line represents the calculation with the original soft-SAFT equation; the full line is the performance of the equation with the crossover treatment. The symbols are the experimental data, Circles are from [43,44]. Squares are from [24].

**Figure 3** Pressure - density diagram of  $N_2O_4$  at 294.3K (top) and 360.9K (bottom). The dashed lines are from the soft-SAFT predictions, full lines are those from the crossover soft-SAFT calculations. Circles are the experimental data [43].

**Figure 4** Temperature dependence of the mole fraction of  $\text{NO}_2$  in the nitrogen dioxide / dinitrogen tetroxide reactive mixture. **a)** vapor - liquid coexistence region; **b)** liquid phase at low temperature. The dashed line represents the calculation with the original soft-SAFT equation; the full line is the performance of the equation with the crossover treatment. Circles are experimental data from [8].

**Figure 5** Comparison between experimental data from [45] and crossover soft-SAFT EoS mole fraction of nitrogen dioxide in the vapor phase in a nitrogen dioxide / dinitrogen tetroxide reaction mixture at 298.5 K.

**Figure 6** Equilibrium constant versus Temperature for the dissociation of nitrogen tetroxide. Symbols are from [46], while lines are the crossover soft-SAFT predictions.

**Figure 7** Pressure –  $\text{CO}_2$  mass fraction diagram of the  $\text{CO}_2 + (\text{NO}_2 / \text{N}_2\text{O}_4)$  mixture at three different temperatures. Symbols are experimental data [29] at ( $\square$ ) 298.15K, ( $\circ$ ) 313.15K and ( $\Delta$ ) 328.45K, while the lines are crossover soft-SAFT predictions. The top line indicates the calculated critical line.

**Table 1** soft-SAFT optimized parameters for the compounds investigated in this work. Three sets of parameters are presented for CO<sub>2</sub>: the original parameters without crossover, obtained by Dias et al [21], the parameters obtained in this work when the crossover term was included, and the same parameters  $m$ ,  $\sigma$  and  $\varepsilon$  values without the crossover term. For the NO<sub>2</sub> system only two sets of parameters were considered, since  $m$ ,  $\sigma$ ,  $\varepsilon$ ,  $\varepsilon^{HB}$  and  $\kappa^{HB}$  had the same values for the two versions of the equation. See text for details.

	$m$	$\sigma$	$\varepsilon/k_B$	$\Phi$	$L$	$Q$	$\varepsilon^{HB}/k_B$	$\kappa^{HB}$	$T_{range}$	% AAD	% AAD
		(Å)	(K)			(C.m <sup>2</sup> )	(K)	(Å <sup>3</sup> )	(K)	P <sub>vap</sub>	$\rho$
CO <sub>2</sub>	1.606	3.174	158.5	5.70	1.130	4.4.10 <sup>-40</sup>	-	-	220-290	0.61	0.94
	1.606	3.174	158.5	-	-	4.4.10 <sup>-40</sup>	-	-	220-290	0.61	0.94
[21]	1.571	3.184	160.2	-	-	4.4.10 <sup>-40</sup>	-	-	220-290	0.50	0.90
NO <sub>2</sub>	1.295	3.200	247.8	6.50	1.172	-	6681	1.0	294-420	0.35	0.22
	1.295	3.200	247.8	-	-	-	6681	1.0	294-420	0.35	0.22

**Table 2** Calculated and experimental critical constant for CO<sub>2</sub> [40] and NO<sub>2</sub> / N<sub>2</sub>O<sub>4</sub> [43]

T <sub>c</sub> (K)				P <sub>c</sub> (MPa)			ρ <sub>c</sub> (mol/L)		
compound	exp.	crossover	soft-SAFT	exp.	crossover	soft-SAFT	exp.	crossover	soft-SAFT
		soft-SAFT			soft-SAFT			soft-SAFT	
CO <sub>2</sub>	304.1	304	324	7.38 <sup>[40]</sup>	7.46	9.76	10.62	10.42	11.25
NO <sub>2</sub>	431.1	431.0	450.0	10.13 <sup>[43]</sup>	9.90	12.82	11.96	11.79	11.21

**Table 3** Variable absolute derivation of the calculated pressure

	T (K)	$\xi_j$	Data no	Data reference	AADP %
CO <sub>2</sub> + NO <sub>2</sub> / N <sub>2</sub> O <sub>4</sub>	298.15	1.045	1	2	0.003
	313.15	1.045	14	2	0.825
	328.45	1.045	3	2	2.200



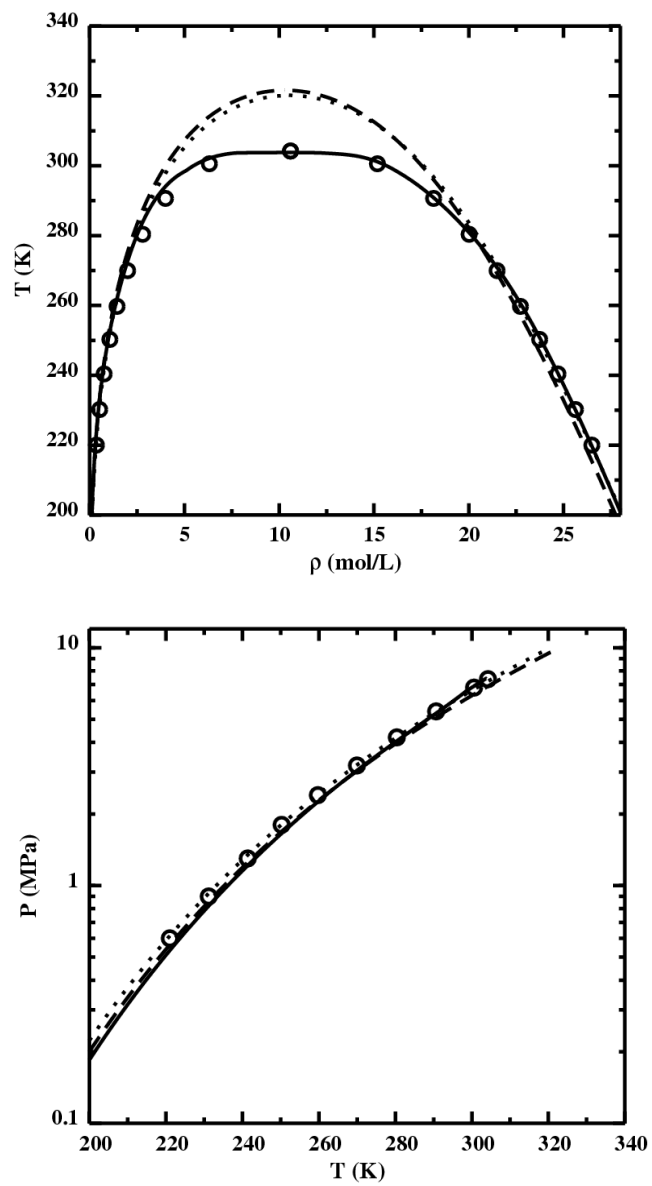


Figure 1: Belkadi et al.

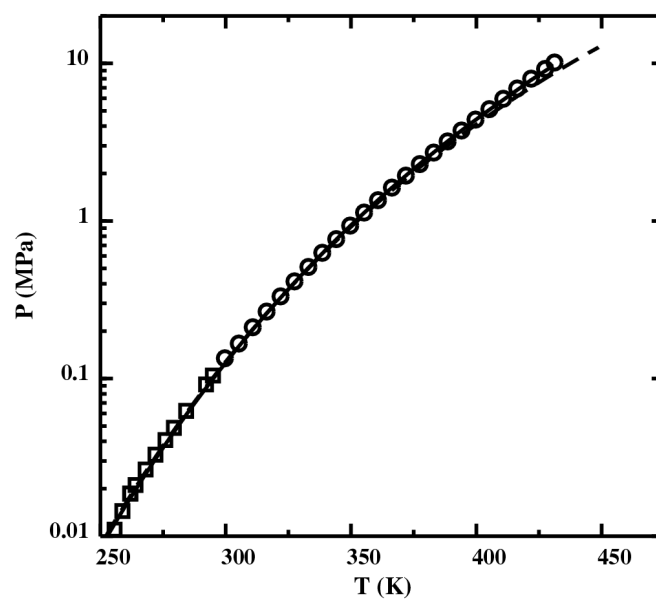
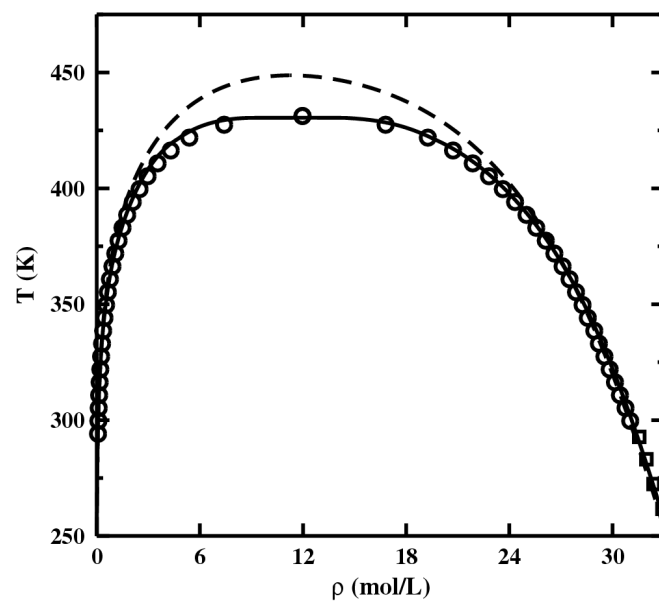


Figure 2: Belkadi et al.

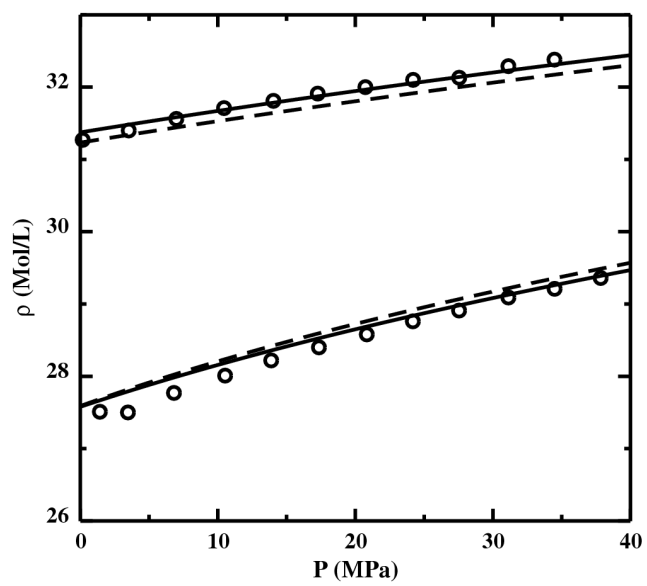


Figure 3: Belkadi et al.

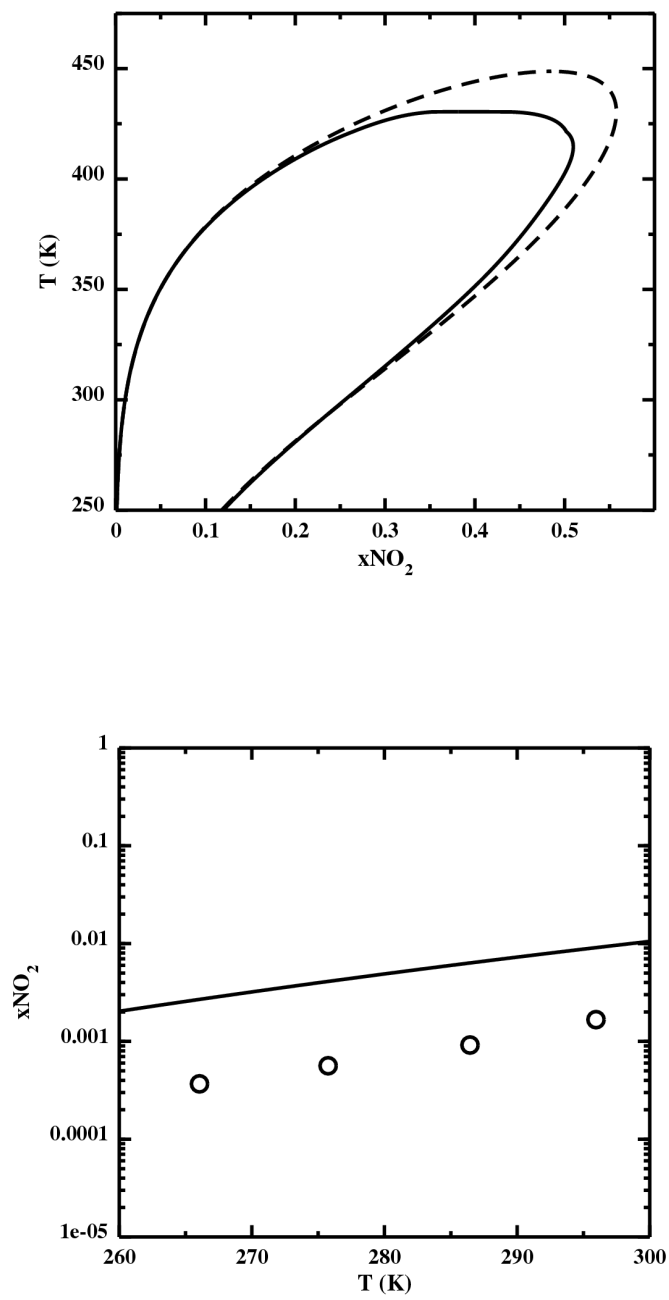


Figure 4: Belkadi et al.

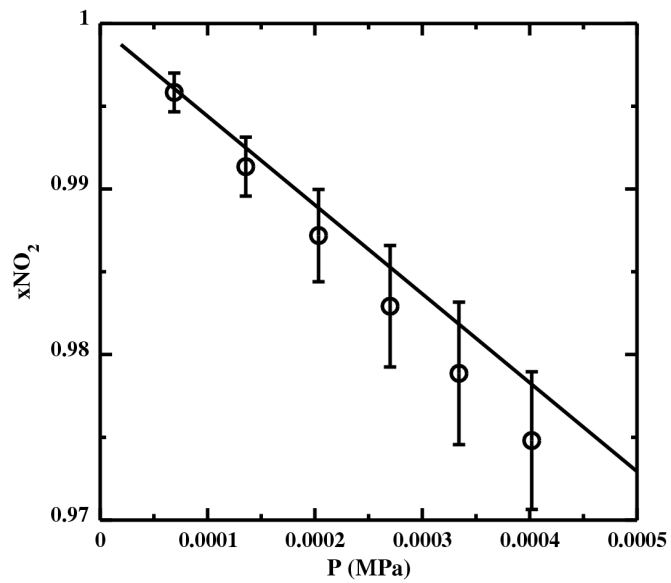


Figure 5: Belkadi et al.

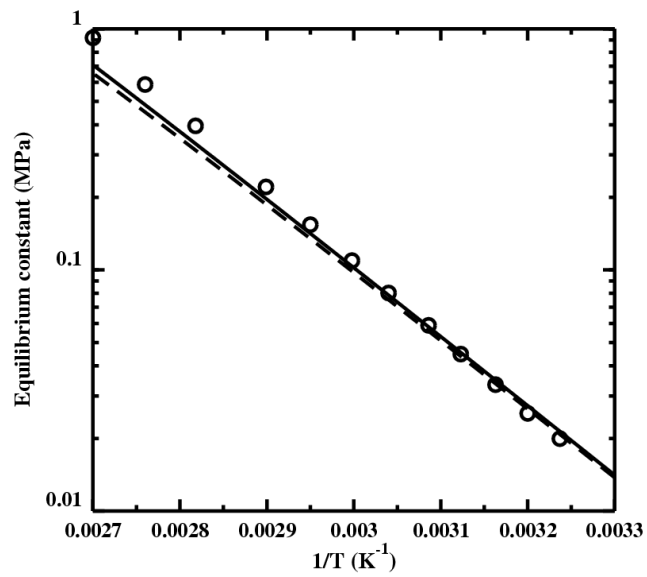


Figure 6: Belkadi et al.

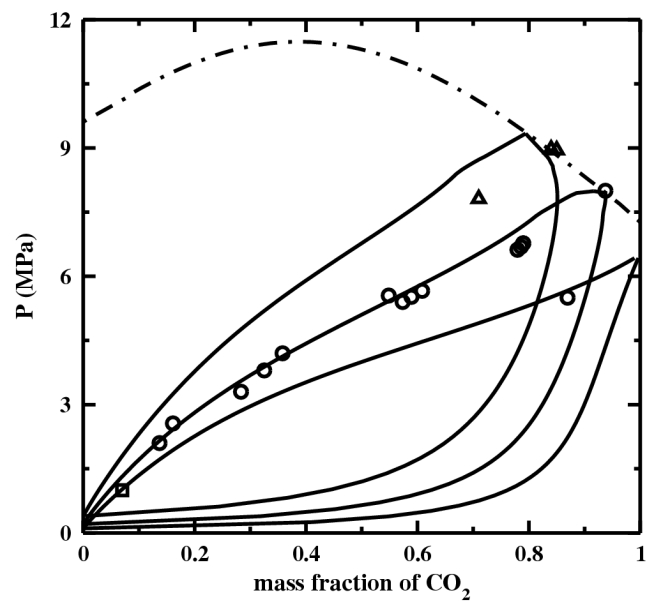


Figure 7: Belkadi et al.